Journal of Hazardous Materials 162 (2009) 1193–1198

Contents lists available at ScienceDirect

Journal of Hazardous Materials

journal homepage: www.elsevier.com/locate/jhazmat

Degradation of nitrobenzene using titania photocatalyst co-doped with nitrogen and cerium under visible light illumination

Xiang-Zhong Shen*, Zhi-Cheng Liu, Shan-Mei Xie, Jun Guo

Department of Chemistry and Materials Science, Hunan Institute of the Humanities and Science and Technology, Loudi 417000, China

ARTICLE INFO

Article history:
Received 5 March 2008
Received in revised form 1 June 2008
Accepted 3 June 2008
Available online 8 June 2008

Keywords:
Nitrobenzene degradation
Nitrogen
Cerium
Co-doped
Titania photocatalysis

ABSTRACT

A type of nitrogen and cerium co-doped titania photocatalyst, which could degrade nitrobenzene under visible light irradiation, was prepared by the sol–gel route. Titanium isopropoxide, ammonium nitrate, and cerium nitrate were used as the sources of titanium, nitrogen, and cerium, respectively. X-ray diffraction (XRD), X-ray photoelectron spectroscopy (XPS), UV–vis diffusive reflectance spectroscopy (DRS), scanning electron microscopy (SEM), and N_2 adsorption–desorption isotherm were employed to characterize the as-prepared photocatalyst. The degradation of nitrobenzene under visible light illumination was taken as probe reaction to evaluate the photoactivity of the co-doped photocatalyst. The commercial TiO_2 photocatalyst (Degussa P25), which was thought as a high active photocatalyst, was chosen as standard photocatalyst to contrast the photoactivity of the nitrogen and cerium co-doped titania photocatalyst. The results showed that the photocatalytic performance of the nitrogen and cerium co-doped titania was related with the calcination temperature and the component. The nitrogen atoms were incorporated into the crystal of titania and could narrow the band gap energy. The doping cerium atoms existed in the forms of Ce_2O_3 and dispersed on the surface of TiO_2. The improvement of the photocatalytic activity was ascribed to the synergistic effects of the nitrogen and cerium co-doping.

1. Introduction

In the past decades, semiconductor photocatalysis has been the focus of numerous studies and TiO_2 is frequently used as photocatalyst to degrade a great deal of pollutants resulting from industrial and agricultural wastes because of its excellent properties [1–5]. However, titania can be activated only by ultraviolet (UV) light because of the high energy band gap (ca. 3.2 eV for anatase) [6,7]. In addition, low photo quantum efficiency and high recombination of electron–hole pairs restrict the application of titania [8–10]. Therefore, all kinds of attempts have been made to improve optical absorption and photocatalytic activity for the purpose of extending the light absorption toward the visible light range and to suppress the recombination of hole–electron pairs, and the most feasible modification methods seem to be doping with metal and doping with nonmetal [9–15].

Previous studies demonstrated that the mechanisms of modification to titania varied with methods. The doping of nonmetal could narrow the band gap and might drive the response to visible light and catalytic activity, whereas the doping of metal could trap temporarily the photogenerated charge carriers and might suppress the recombination of photo-induced electron–hole pairs when migrating from the inside of the photocatalyst to the surface [6,7,9,10,13–19].

The modification to titania by co-doping was an effective method and the cooperate action of the co-doping was able to improve the photocatalytic activity. Yuan et al. [20] reported that the cooperative action of co-doping of Zn^{2+} and Fe^{3+} over titania could obviously improve the photocatalytic performance for the phenol degradation. Zhao et al. [21] prepared the B–Ni co-doped photocatalyst using the modified sol–gel method. They pointed out that incorporation of B into TiO_2 could extend the spectral response to the visible region and that Ni doping could increase greatly the photocatalytic activity. Lin et al. [22] prepared the N–P co-doped titania photocatalyst extending spectral response to the visible light region. They proved that co-doping of both N and P could improve significantly the photocatalytic activity under both UV light and visible light. Balek et al. [23] reported that the nitrogen and fluorine co-doped titania photocatalyst showing high photocatalytic activity in a visible region of spectrum for acetaldehyde decomposition was prepared by spray pyrolysis using a mixed solution of $TiCl_4$ and NH_4F. They demonstrated that the observed high photocatalytic activity of the samples could be ascribed to a synergetic effect of nitrogen and fluorine co-doping. Ling et al. [24] prepared the B and N co-doped TiO_2 nanopowders using boric acid and ammonium fluoride as the precursors of boron and nitrogen. They proved

* Corresponding author. Tel.: +86 738 8325200; fax: +86 738 8325200.
E-mail address: ldsz0738@163.com (X.-Z. Shen).

0304-3894/$ – see front matter © 2008 Elsevier B.V. All rights reserved.
doi:10.1016/j.jhazmat.2008.06.004

that the synergistic effect of B and N co-doping was responsible for improving the photocatalytic performance. These reports unequivocally indicated that modification to titania by co-doping was an effective method for increasing the photocatalytic activity.

However, there were few reports on the co-doped photocatalyst with nitrogen and cerium. In the present work, the nitrogen and cerium co-doped titania photocatalyst with high photocatalytic performance under visible light was prepared using the sol–gel method. The prepared samples were characterized by XRD, XPS, DRS, SEM, and N_2 adsorption–desorption isotherm. The photocatalytic performance was evaluated by means of the degradation for nitrobenzene under visible light illumination.

2. Experimental

2.1. Photocatalyst preparation

In this study titanium isopropoxide was chemically pure and others were analytically pure. All chemicals were used without any further purification. Water used was deionized water.

The nitrogen and cerium co-doped titania was synthesized by the following procedure. A certain amount of ammonium nitrate and cerium nitrate was dissolved in the mixture of 10 mL of deionized water, 10 mL of glacial acetic acid, and 80 mL of ethanol at room temperature to gain solution A. Titanium isopropoxide (28.6 g, 0.1 mol) was dissolved in 100 mL of absolute ethanol to form solution B. Then, the solution B was added drop-wise into the solution A within 60 min under vigorous stirring, followed by stirring for 2 h. The resulting sol was aged for 48 h at room temperature and was dried for 12 h at 80 °C. Thus, the xerogel was to be obtained. The resultant xerogel was milled and annealed at different temperature for 3 h to remove the residual organic compounds to prepare the nitrogen and cerium co-doped photocatalyst. The sample was labeled as N(x)Ce(y)TiO_2-t, where x and y represented the mole ratios of ammonium nitrate to titanium isopropoxide and cerium nitrate to titanium isopropoxide, respectively, and t denoted the corresponding temperature of calcination (°C).

2.2. Photocatalyst characterization

The XRD patterns of samples were recorded by means of a D/max-RB X-ray diffractometer equipped with Cu Kα radiation (λ = 0.15406 nm) in a 2θ range of 20–70°. The scanning speed was 4°/min. The standard diffraction charts of anatase and rutile were used to compare with the obtaining XRD patterns. Crystallite sizes of the samples were estimated by the Scherrer equation and the lattice constants were calculated using full profile structure refinement of XRD data. The X-ray photoelectron spectra of the co-doped photocatalyst were measured by a Thermo Escalab250 X-ray photoelectron spectroscope equipped with Al Kα excitation. The binding energies for N 1s, Ti 2p, and Ce 3d were calibrated with respect to the signal for adventitious carbon (binding energy = 284.6 eV). The surface electronic states and the chemical states were analyzed using the binding energies. The UV–vis diffusive reflectance absorption spectra of samples were recorded on a Shimadzu (Japan) UV–Vis 2100S spectrophotometer with an integrating sphere attachment. The scanning range was between 200 nm and 800 nm. $BaSO_4$ was used as a reference. The structural morphology of sample was observed by a microscope (Philips XL 30 CP). The particle size was estimated approximately by SEM photograph. Specific surface area was determined by the BET method based N_2 adsorption on a Autosorb-1 at 77 K. Prior to adsorption measurement, the sample was degassed in an evacuation chamber for 12 h at 423 K.

2.3. Photocatalytic activity test

Nitrobenzene was used as a model organic pollutant. The degradation of nitrobenzene was taken as a model reaction to assess the photocatalytic performance of the nitrogen and cerium co-doped titania photocatalyst. In all the studies, the suspension containing 200 mL of 50 mg/L nitrobenzene aqueous solution and 0.20 g of photocatalyst was loaded in a 500 mL of homemade quartz vessel beaker and was magnetically stirred. A 300 W xenon lamp provided the light source and a 400 nm glass filter was used to remove the UV light. The degradation reaction was carried out under visible light irradiation and the reaction temperature was maintained at 30.0 °C. After the mixture was ultrasonicated for 10 min and stirred for 60 min in the dark to achieve the adsorption equilibrium, the xenon lamp was turned on. The decomposition experiment was carried out for 4 h. Prior to irradiation and after irradiation of 4 h, 5 mL of sample was taken out and centrifugated for determining the nitrobenzene concentration, from which the nitrobenzene conversion was calculated.

3. Results and discussion

3.1. XRD spectra of samples

Fig. 1 shows the XRD patterns of the different samples. From Fig. 1, one could observe a characteristic peak (2θ = 27.4°) assigned to rutile (1 1 0) for the sample TiO_2-600. However, one could not see the characteristic peak assigned to rutile for the other samples. One could conclude that the sample TiO_2-600 existed in the states of both anatase and rutile, and that the other samples existed only in anatase phase. Obviously, the XRD patterns revealed that the doping could retard the transformation from anatase to rutile at elevated temperatures. According to the previous literatures [17,25–28], the N doping can make the prepared sample more porous, corresponding to the larger BET surface area; the Ce doping can lead to the well-crystallized anatase mesostructure, thus increasing the crystallization temperature of the titania powder and inhibited the phase transformation of anatase to rutile.

According to Fig. 1, the width of the (1 0 1) plane diffraction peak of anatase (2θ = 25.3°) become narrower for the nitrogen and cerium co-doped titania with the annealing temperature increasing. Based on the Scherrer equation, one could conclude that the average particle size increased when increasing the calcination

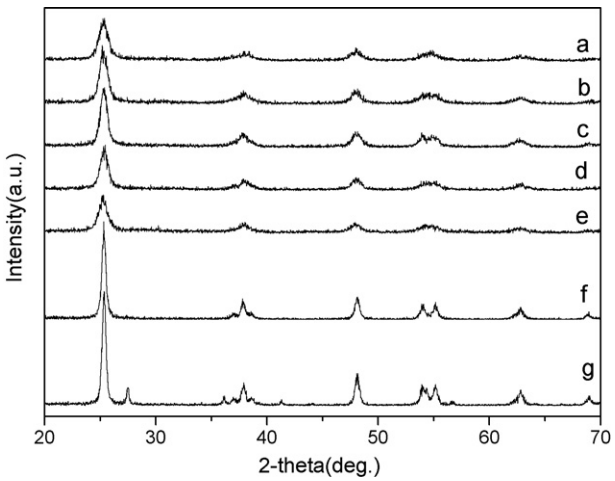

Fig. 1. XRD patterns of different samples: (a) N(0.02)Ce(0.01)TiO_2-400, (b) N(0.02)Ce(0.01)TiO_2-500, (c) N(0.02)Ce(0.01)TiO_2-600, (d) N(0.02)TiO_2-500, (e) Ce(0.01)TiO_2-500, (f) TiO_2-500, and (g) TiO_2-600.

Table 1
Crystal size and surface area of samples

Sample	Crystal size (nm)	Surface area (m^2/g)
TiO_2-500	22.9	29.8
Ce(0.01)TiO_2-500	10.8	89.6
N(0.02)Ce(0.01)TiO_2-400	9.2	151.9
N(0.02)Ce(0.01)TiO_2-500	9.6	144.5
N(0.02)Ce(0.01)TiO_2-600	10.2	132.7

Table 2
Crystal constants of the typical samples

Sample	$a = b$ (nm)	c (nm)
TiO_2-500	0.37825	0.95119
Ce(0.01)TiO_2-500	0.37848	0.95136
N(0.02)TiO_2-500	0.37806	0.94835
N(0.02)Ce(0.01)TiO_2-500	0.37817	0.94862

temperature. Moreover, the average grain sizes of the samples were shown in Table 1 and were 22.9 nm, 9.2 nm, 9.6 nm, and 10.2 nm for TiO_2-500, N(0.02)Ce(0.01)TiO_2-400, N(0.02)Ce(0.01)TiO_2-500, and N(0.02)Ce(0.01)TiO_2-600, respectively. Apparently, the annealing temperature had an effect on the grain size of the nitrogen and cerium co-doped titania photocatalyst.

The lattice constants of the typical samples were measured and were used to determine whether the doping atoms could incorporate into TiO_2 lattice. Table 2 shows the lattice parameters of the samples. Compared with the lattice parameters of TiO_2-500, the corresponding values of the sample Ce(0.01)TiO_2-500 were almost unchanged. The lattice parameters a and b of the samples N(0.02)TiO_2-500 and N(0.02)Ce(0.01)TiO_2-500 remained almost unvaried while the c parameters decreased. This indicated that the crystal lattices of the two samples were locally destroyed by N doping. The above results revealed that nitrogen atoms were incorporated into the crystal lattice of TiO_2 whereas cerium atoms were not incorporated into TiO_2.

3.2. XPS spectra of the nitrogen and cerium co-doped TiO_2 photocatalyst

The XPS spectra of the typical sample N(0.02)Ce(0.01)TiO_2-500 for N 1s, Ti 2p, and Ce 3d are shown in Figs. 2–4, respectively. The binding energy (BE) for N 1s was 397.0 eV in TiN [29] and BE for Ti $2p_{3/2}$ in TiN was 455.2 eV [30]. According to Figs. 2 and 3, BE for N 1s

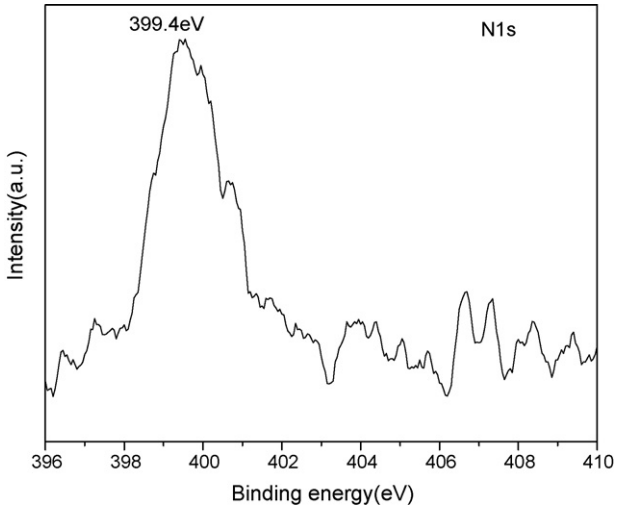

Fig. 2. XPS spectra of the typical sample N(0.02)Ce(0.01)TiO_2-500 for N 1s.

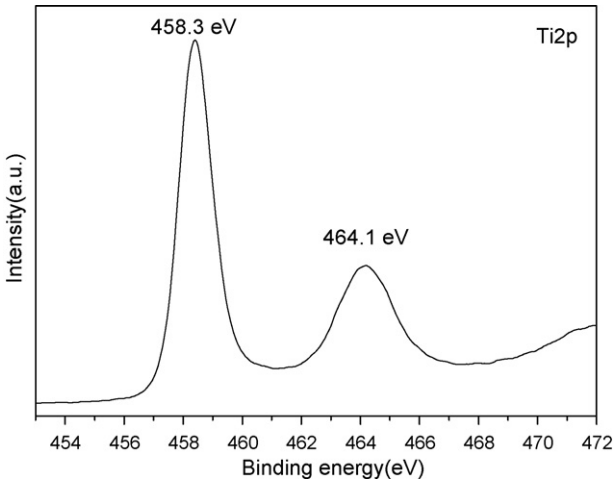

Fig. 3. XPS spectra of the typical sample N(0.02)Ce(0.01)TiO_2-500 for Ti 2p.

was 399.4 eV, and the binding energies (BEs) for Ti 2p were 458.3 eV and 464.1 eV. These results demonstrated that there was no existence of the compound TiN, and further confirmed that nitrogen atoms (BE = 399.4 eV) in the sample N(0.02)Ce(0.01)TiO_2-500 had been doped into TiO_2 lattice. This accorded well with the result from XRD analysis. BEs for Ti 2p at 458.3 eV and 464.1 eV were assigned to Ti $2p_{3/2}$ and Ti $2p_{1/2}$ of TiO_2. BE for Ce 3d in Ce_2O_3 was 885.8 eV [31]. Fig. 4 revealed that BE for Ce 3d was 885.7 eV, which should be attributed to Ce $3d_{5/2}$ in Ce_2O_3. From Fig. 4, one concluded that cerium nitrate was changed into Ce_2O_3 by annealing. Therefore, the doping Ce existed in the form of Ce_2O_3. In fact, the ionic radii of Ce^{3+} and Ti^{4+} are 0.101 nm, 0.068 nm, respectively. It was not difficult to understand that Ce^{3+} could not be incorporated into the lattice of TiO_2.

Combined with the XRD analysis, one could deduce that the doping nitrogen atoms were weaved into titania crystals, and that the doping cerium atoms presented in the forms of Ce_2O_3 and were distributed on the surface of titania.

3.3. UV–vis DRS spectra of samples

Fig. 5 shows the optical absorption spectra of the different samples. The samples N(0.02)TiO_2-500 and N(0.02)Ce(0.01)TiO_2-500 absorbed observably in the visible region from 400 nm to 800 nm

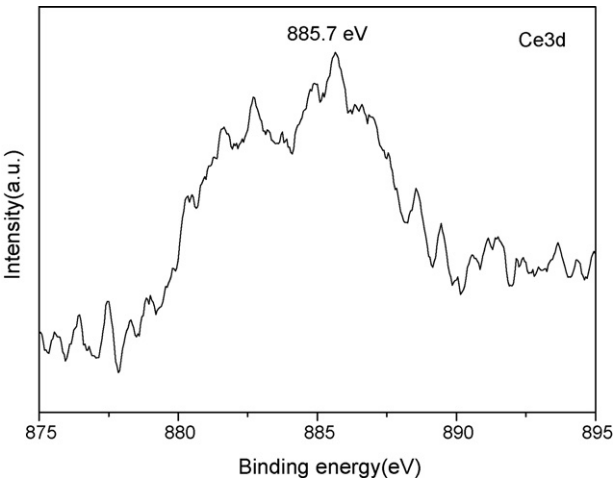

Fig. 4. XPS spectra of the typical sample N(0.02)Ce(0.01)TiO_2-500 for Ce 3d.

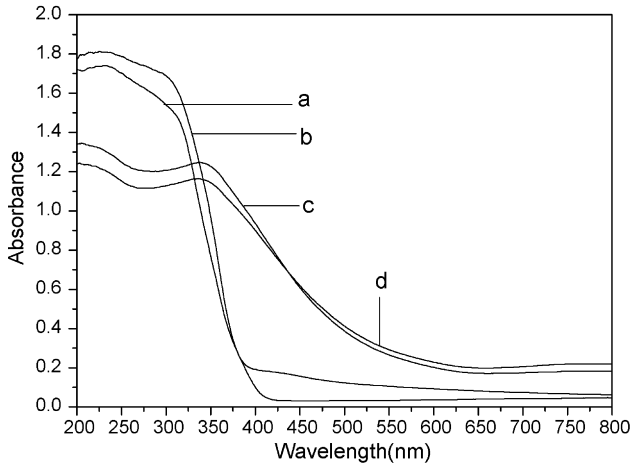

Fig. 5. Diffuse reflectance absorption spectra of the different samples: (a) TiO_2-500, (b) Ce(0.01)TiO_2-500, (c) N(0.02)TiO_2-500, and (d) N(0.02)Ce(0.01)TiO_2-500.

wavelengths. However, the samples Ce(0.01)TiO_2-500 and TiO_2-500 hardly absorbed visible light. The red shift of the absorption edge demonstrated a decrease in the band gap energy. According to the results from XRD and XPS, the doping nitrogen atoms were weaved into titania crystals and led to the modification of the electronic structure around the conduction band edge of TiO_2 because of the substitution of the lattice oxygen by nitrogen during the TiO_2 nitridation, whereas the doping cerium atoms presented in the forms of Ce_2O_3 and were distributed on the surface of titania. Therefore, N doping led to the band gap narrowing [17]. However, Ce doping did not.

Furthermore, the intercept on the wavelength axis for a tangent drawn on DRS spectra was used to determine the onsets of absorption edge, which were 393.1 nm for TiO_2-500 and 560.7 nm for the sample N(0.02)Ce(0.01)TiO_2-500.

3.4. SEM photograph of N–Ce co-doped TiO_2 photocatalyst

Fig. 6 shows SEM photograph of the typical sample N(0.02)Ce(0.01)TiO_2-500. From the image, the sample N(0.02)Ce(0.01)TiO_2-500 existed approximately in the form of spherical particle and presented the porous structures. According to the statistical estimation, the average size was about 10.3 nm, which was in accordance with the value determined by XRD (9.6 nm). In addition, other samples investigated were so from the SEM images (not shown), too.

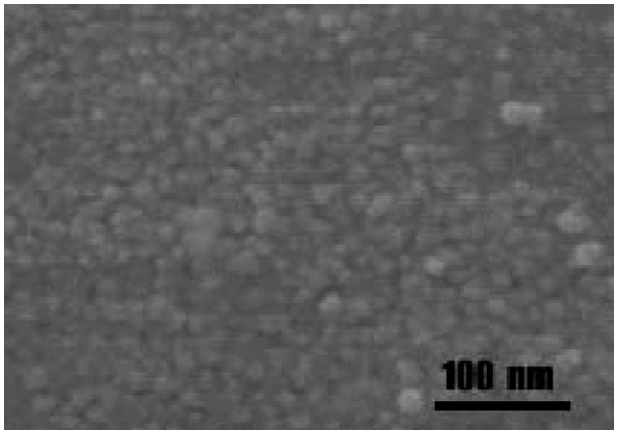

Fig. 6. SEM pattern of the typical sample N(0.02)Ce(0.01)TiO_2-500.

Table 3
The concentrations of nitrobenzene at the adsorption equilibrium after 60 min in the dark over different photocatalysts

Sample	C_{in} (mg/mL)	C_0 (mg/mL)
P25	50.00	42.06
N(0.02)Ce(0.01)TiO_2-500	50.00	38.48
N(0.02)TiO_2-500	50.00	41.30
Ce(0.01)TiO_2-500	50.00	44.68
TiO_2-500	50.00	45.92
N(0.02)Ce(0.01)TiO_2-400	50.00	38.39
N(0.02)Ce(0.01)TiO_2-450	50.00	38.75
N(0.02)Ce(0.01)TiO_2-550	50.00	39.02
N(0.02)Ce(0.01)TiO_2-600	50.00	39.35
N(0.02)Ce(0.005)TiO_2-500	50.00	40.03
N(0.02)Ce(0.02)TiO_2-500	50.00	39.55
N(0.01)Ce(0.01)TiO_2-500	50.00	39.85
N(0.025)Ce(0.01)TiO_2-500	50.00	39.78

C_{in}: the initial concentration. C_0: the concentration at the adsorption equilibrium.

3.5. BET surface area

Table 1 shows the Brunauer–Emmett–Teller (BET) surface areas of different samples calculated from the linear part of the BET plots. The surface areas were 29.8 m^2/g, 89.6 m^2/g, 151.9 m^2/g, 144.5 m^2/g, and 132.7 m^2/g for the samples TiO_2-500, Ce(0.01)TiO_2-500, N(0.02)Ce(0.01)TiO_2-400, N(0.02)Ce(0.01)TiO_2-500, and N(0.02)Ce(0.01)TiO_2-600, respectively. There was no doubt that co-doping led to the increase of BET surface area. In addition, the annealing temperature had an effect on the surface area of the nitrogen and cerium co-doped photocatalyst. As is well known, the photocatalytic reaction occurs on the surface and the surface area of photocatalyst influences the photocatalytic rate.

3.6. Photocatalytic performance

The adsorption of target pollutant over photocatalyst is the prerequisite of photocatalysis. Table 3 shows the concentrations of nitrobenzene at the adsorption equilibrium after 60 min in the dark over different photocatalysts. Obviously, it could be seen that the adsorption of nitrobenzene over different photocatalysts was influenced by the annealing temperatures and the component, and that the sample N(0.02)Ce(0.01)TiO_2-400 adsorbed the most amount of nitrobenzene at the adsorption equilibrium among these samples. Fig. 7 shows the nitrobenzene conversion within 4 h under visible illumination over the different samples including P25,

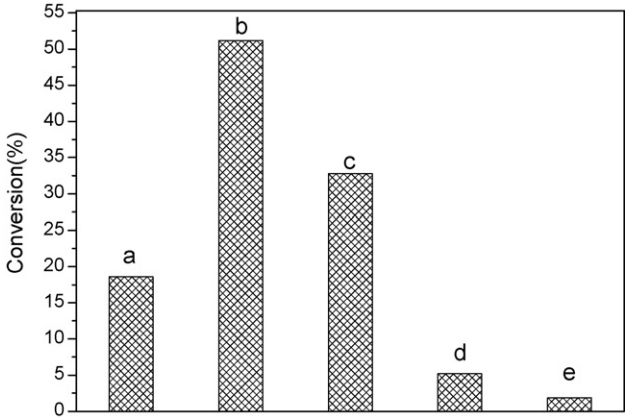

Fig. 7. The nitrobenzene conversion within 4 h under visible illumination over the different samples: (a) P25, (b) N(0.02)Ce(0.01)TiO_2-500, (c) N(0.02)TiO_2-500, (d) Ce(0.01)TiO_2-500, and (e) TiO_2-500.

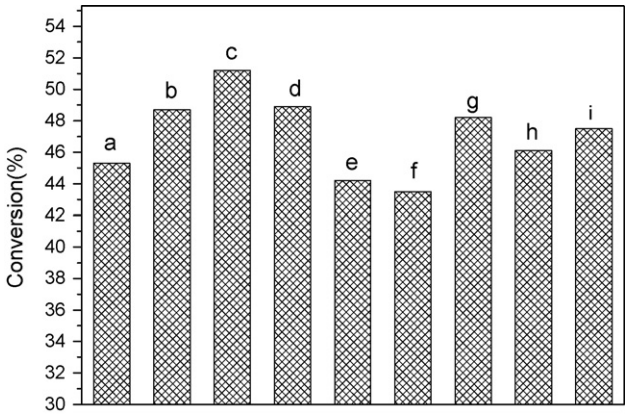

Fig. 8. The nitrobenzene conversion within 4 h under visible illumination over the N–Ce co-doped titania samples with the different annealing temperatures and with the different component: (a) N(0.02)Ce(0.01)TiO_2-400, (b) N(0.02)Ce(0.01)TiO_2-450, (c) N(0.02)Ce(0.01)TiO_2-500, (d) N(0.02)Ce(0.01)TiO_2-550, (e) N(0.02)Ce(0.01)TiO_2-600, (f) N(0.02)Ce(0.005)TiO_2-500, (g) N(0.02)Ce(0.02)TiO_2-500, (h) N(0.01)Ce(0.01)TiO_2-500, and (i) N(0.025)Ce(0.01)TiO_2-500.

N(0.02)Ce(0.01)TiO_2-500, N(0.02)TiO_2-500, Ce(0.01)TiO_2-500, and TiO_2-500. Obviously, the samples P25, N(0.02)Ce(0.01)TiO_2-500, and N(0.02)TiO_2-500 exhibited photocatalytic activity under visible light irradiation, whereas the samples Ce(0.01)TiO_2-500 or TiO_2-500 hardly degraded nitrobenzene. The results were in agreement with the outcome from the DRS analysis. According to Fig. 7, the photocatalytic activity of N(0.02)Ce(0.01)TiO_2-500 was superior to that of N(0.02)TiO_2-500, indicating that Ce_2O_3 distributed on the surface of photocatalyst doped with N could further improve the photocatalytic performance. It could be observed that the photoactivity of N(0.02)Ce(0.01)TiO_2-500 exceeded that of P25. Compared with P25, there was an increase of 175% in photoactivity for the decomposing nitrobenzene under visible light for the sample N(0.02)Ce(0.01)TiO_2-500.

Fig. 8 shows the nitrobenzene conversion within 4 h under visible illumination over the nitrogen and cerium co-doped titania samples with the different annealing temperatures and with the different component, including N(0.02)Ce(0.01)TiO_2-400, N(0.02)Ce(0.01)TiO_2-450, N(0.02)Ce(0.01)TiO_2-500, N(0.02)Ce(0.01)TiO_2-550, N(0.02)Ce(0.01)TiO_2-600, N(0.01)Ce(0.01)TiO_2-500, N(0.015)Ce(0.01)TiO_2-500, N(0.025)Ce(0.01)TiO_2-500, N(0.02)Ce(0.005)TiO_2-500, and N(0.02)Ce(0.02)TiO_2-500. All the nitrogen and cerium co-doped titania samples showed photocatalytic activity under visible light irradiation. Compared with the nitrobenzene conversions over these samples, one could deduce that the photoactivity of the nitrogen and cerium co-doped titania photocatalyst was related to the annealing temperatures, and that the component of photocatalyst influenced the photoactivity. Among these samples, N(0.02)Ce(0.01)TiO_2-500 owned the best photocatalytic performance for the nitrobenzene degradation within 4 h. It has been widely accepted that many factors have effects on the photoactivity of photocatalyst and these factors are closely related to each other [19,32–34]. Therefore, it was easy to understand that the sample N(0.02)Ce(0.01)TiO_2-500 exhibited the highest photocatalytic performance for nitrobenzene decomposition under visible light illumination.

In order to test the stability of the nitrogen and cerium co-doped titania photocatalyst, six cycles of photocatalytic experiments were done using the sample N(0.02)Ce(0.01)TiO_2-500 under visible irradiation. The photoactivity was found not to decrease, demonstrating that the as-prepared titania photocatalyst co-doped with nitrogen and cerium was stable.

4. Conclusions

The nitrogen and cerium co-doped titania photocatalyst was prepared through the sol–gel route. The as-prepared photocatalyst could adsorb the visible light and showed high photoactivity in the visible region because of the band gap narrowing. Nitrogen atoms were incorporated into the crystal lattice of titania and nitrogen doping destroyed locally the crystal structure, resulting in the response to the visible light. Cerium atoms existed in the state of Ce_2O_3 and were dispersed on the surface of titania, suppressing the recombination of electron–hole pairs and increasing the photoactivity. The as-prepared titania photocatalyst presented approximately the spherical shape and owned the porous surface. The average crystal size and the surface area correlated with the calcination temperature. The catalytic performance was influenced by the annealing temperature and the component of photocatalyst. The cooperative effect of the nitrogen and cerium co-doping improved the photocatalytic activity. The photoactivity of the as-prepared titania photocatalyst co-doped with nitrogen and cerium exceeded that of P25 for the decomposing nitrobenzene under visible light.

References

[1] M.R. Hoffmann, S.T. Martin, W. Choi, D.W. Bahneman, Environmental applications of semiconductor photocatalysis, Chem. Rev. 95 (1995) 69–96.
[2] J. Matos, J. Laine, J.M. Herrmann, Synergy effect in the photocatalytic degradation of phenol on a suspended mixture of titania and activated carbon, Appl. Catal. B 18 (1998) 281–291.
[3] K. Hashimoto, H. Irie, A. Fujishima, TiO_2 photocatalysis: a historical overview and future prospects, Jpn. J. Appl. Phys. 44 (2005) 8269–8285.
[4] R.J. Tayade, R.G. Kulkarni, R.V. Jasra, Photocatalytic degradation of aqueous nitrobenzene by nanocrystalline TiO_2, Ind. Eng. Chem. Res. 45 (2006) 922–927.
[5] L. Reijnders, Hazard reduction for the application of titania nanoparticles in environmental technology, J. Hazard. Mater. 152 (2008) 440–445.
[6] R. Asahi, T. Morikawa, T. Ohwaki, K. Aoki, Y. Taga, Visible-light photocatalysis in nitrogen-doped titanium oxides, Science 293 (2001) 269–271.
[7] T. Ohno, M. Akiyoshi, T. Umebayashi, K. Asai, T. Mitsui, M. Matsumura, Preparation of S-doped TiO_2 photocatalysts and their photocatalytic activities under visible light, Appl. Catal. A 265 (2004) 115–121.
[8] E. Borgarello, J. Kiwi, M. Gratzel, E. Pelizzetti, M. Visca, Visible light induced water cleavage in colloidal solutions of chromium-doped titanium dioxide particles, J. Am. Chem. Soc. 104 (1982) 2996–3002.
[9] A.W. Xu, Y. Gao, H.Q. Liu, The preparation, characterization, and their photocatalytic activities of rare-earth-doped TiO_2 nanoparticles, J. Catal. 207 (2002) 151–157.
[10] W. Choi, A. Termin, M.R. Hoffmann, The role of metal ion dopants in quantum-sized TiO_2: correlation between photoreactivity and charge carrier recombination dynamics, J. Phys. Chem. 98 (1994) 13669–13679.
[11] M. Anpo, M. Takeuchi, The design and development of highly reactive titanium oxide photocatalysts operating under visible light irradiation, J. Catal. 216 (2003) 505–516.
[12] H.M. Zhang, X. Quan, S. Chen, H.M. Zhao, Fabrication and characterization of silica/titania nanotubes composite membrane with photocatalytic capability, Environ. Sci. Technol. 40 (2006) 6104–6109.
[13] S. Sakthivel, H. Kisch, Daylight photocatalysis by carbon-modified titanium dioxide, Angew. Chem. Int. Ed. 42 (2003) 4908–4911.
[14] Y. Wang, H. Cheng, L. Zhang, Y.Z. Hao, J.M. Ma, B. Xu, W.H. Li, The preparation, characterization, photoelectrochemical and photocatalytic properties of lanthanide metal-ion-doped TiO_2 nanoparticles, J. Mol. Catal. A 151 (2000) 205–216.
[15] L. Lin, W. Lin, J.L. Xie, Y.X. Zhu, B.Y. Zhao, Y.C. Xie, Photocatalytic properties of phosphor-doped titania nanoparticles, Appl. Catal. B 75 (2007) 52–58.
[16] M. Mrowetz, W. Balcerski, A.J. Colussi, M.R. Hoffmann, Oxidative power of nitrogen-doped TiO_2 photocatalysts under visible illumination, J. Phys. Chem. B 108 (2004) 17269–17273.
[17] H.X. Li, J.X. Li, Y.N. Huo, Highly active TiO_2N photocatalysts prepared by treating TiO_2 precursors in NH_3/ethanol fluid under supercritical conditions, J. Phys. Chem. B 110 (2006) 1559–1565.
[18] R. Jothiramalingam, M.K. Wang, Synthesis, characterization and photocatalytic activity of porous manganese oxide doped titania for toluene decomposition, J. Hazard. Mater. 147 (2007) 562–569.
[19] J. Lin, J.C. Yu, An investigation on photocatalytic activities of mixed TiO_2-rare earth oxides for the oxidation of acetone in air, J. Photochem. Photobiol. A: Chem. 116 (1998) 63–67.

[20] Z.H. Yuan, J.H. Jia, L.D. Zhang, Influence of co-doping of Zn(II) + Fe(III) on the photocatalytic activity of TiO_2 for phenol degradation, Mater. Chem. Phys. 73 (2002) 323–326.
[21] W. Zhao, W.H. Ma, C.C. Chen, J.C. Zhao, Z.G. Shuai, Efficient degradation of toxic organic pollutants with $Ni_2O_3/TiO_{2-x}B_x$ under visible irradiation, J. Am. Chem. Soc. 126 (2004) 4782–4783.
[22] L. Lin, R.Y. Zheng, J.L. Xie, Y.X. Zhu, Y.C. Xie, Synthesis and characterization of phosphor and nitrogen co-doped titania, Appl. Catal. B 76 (2007) 196–202.
[23] V. Balek, D. Li, J. Subrt, E. Vecernıkova, S. Hishita, T. Mitsuhashi, H. Haneda, Characterization of nitrogen and fluorine co-doped titania photocatalyst: effect of temperature on microstructure and surface activity properties, J. Phys. Chem. Solids 68 (2007) 770–774.
[24] Q.C. Ling, J.Z. Sun, Q.Y. Zhou, Preparation and characterization of visible-light-driven titania photocatalyst co-doped with boron and nitrogen, Appl. Surf. Sci. 254 (2008) 3236–3241.
[25] L.H. Edelson, A.M. Glaeser, Role of particle substructure in the sintering of monosized titania, J. Am. Ceram. Soc. 71 (1988) 225–235.
[26] J.R. Xiao, T.Y. Peng, R. Li, Z.H. Peng, C.H. Yan, Preparation, phase transformation and photocatalytic activities of cerium-doped mesoporous titania nanoparticles, J. Solid State Chem. 179 (2006) 1161–1170.
[27] Y.-H. Xu, H.-R. Chen, Z.-X. Zeng, B. Lei, Investigation on mechanism of photocatalytic activity enhancement of nanometer cerium-doped titania, Appl. Surf. Sci. 252 (2006) 8565–8570.
[28] L. Lin, R.Y. Zheng, J.L. Xie, Y.X. Zhu, Y.C. Xie, Synthesis and characterization of phosphor and nitrogen co-doped titania, Appl. Catal. B: Environ. 76 (2007) 196–202.
[29] S. Badrinarayanan, S. Sinha, A.B. Mandale, XPS studies of nitrogen ion implanted zirconium and titanium, J. Electron Spectrosc. Relat. Phenom. 49 (1989) 303–309.
[30] B.M. Biwer, S.L. Bernasek, Electron spectroscopic study of the iron surface and its interaction with oxygen and nitrogen, J. Electron Spectrosc. Relat. Phenom. 40 (1986) 339–351.
[31] G. Praline, B.E. Koel, R.L. Hance, H.I. Lee, J.M. White, X-ray photoelectron study of the reaction of oxygen with cerium, J. Electron Spectrosc. Relat. Phenom. 21 (1980) 17–30.
[32] G. Colon, M.C. Hidalgo, J.A. Navio, Photocatalytic behaviour of sulphated TiO_2 for phenol degradation, Appl. Catal. B 45 (2003) 39–50.
[33] C. Xie, Q. Yang, Z. Xu, X. Liu, Y. Du, New route to synthesize highly active nanocrystalline sulfated titania-silica: synergetic effects between sulfate species and silica in enhancing the photocatalysis efficiency, J. Phys. Chem. B 110 (2006) 8587–8592.
[34] J. Lukáč, M. Klementová, P. Bezdička, S. Bakardjieva, J. Šubrt, L. Szatmáry, Z. Bastl, J. Jirkovský, Influence of Zr as TiO_2 doping ion on photocatalytic degradation of 4-chlorophenol, Appl. Catal. B 74 (2007) 83–91.